Pergamon

Marine Pollution Bulletin, Vol. 36, No. 12, pp. 961–970, 1998

Printed in Great Britain
0025-326X/98/$19.00+0.00

PII: S0025-326X(98)00006-4

The Relationship Between Oil Droplet Size and Upper Ocean Turbulence

MING LI* and CHRIS GARRETT
Centre for Earch and Ocean Research, University of Victoria, Victoria B.C., Canada V8W 2Y2

Oil spilled at sea often forms oil droplets in stormy conditions. This paper examines possible mechanisms which generate the oil droplets. When droplet Reynolds numbers are large, the dynamic pressure force of turbulent flows is the cause of droplet breakup. Using dimensional analysis, Hinze (1955, *A.I.Ch.E. Journal* 1, 289–295) obtained a formula for the maximum size of oil droplets that can survive the pressure force. When droplet Reynolds numbers are small, however, viscous shear associated with small turbulent eddies is the cause of breakup. For the shear mechanism, we obtain estimates of droplet size as a function of energy dissipation rate, the ratio of oil-to-water viscosity and the surface tension coefficient.

The two formulae are applied to oil spills in the ocean. At dissipation rates expected in breaking waves, the pressure force is the dominant breakup mechanism and can generate oil droplets with radii of hundreds of microns. However, when chemical dispersants are used to treat an oil slick and significantly reduce the oil–water interfacial tension, viscous shear is the dominant breakup mechanism and oil droplets with radii of tens of microns can be generated. Viscous shear is also the mechanism for disintegrating water-in-oil emulsions and the size of a typical emulsion blob is estimated to be tens of millimeters. © 1998 Elsevier Science Ltd. All rights reserved

When oil is accidently spilled into the ocean, it forms a thin film of oil that spreads under the action of gravitational, viscous and surface tension forces (Hoult, 1972). In the presence of surface waves and upper ocean turbulence, however, the oil film can disintegrate, giving rise to small oil droplets or water-in-oil emulsions.

Evaporation, emulsification, and natural dispersion of oil droplets are the three most important factors in determining spilled oil behaviour (Fingas, 1994). Both emulsion formation and droplet dispersion involve a process in which small droplets of one phase are created and dispersed into the second phase (Schramm, 1992). Provided that a sufficient amount of mechanical energy is available, the formation of water-in-oil emulsions as opposed to oil droplets seems to be determined mainly by the chemical composition of the oil. Oil constituents such as asphaltenes and resins behave like lipophilic surfactants when precipitating out as solid particles and can act as emulsifying agents for water-in-oil emulsions when their percentage exceeds about 3% (Bobra *et al.*, 1992).

It is important to know the sizes of oil droplets and blobs of water-in-oil emulsions. As shown in Fig. 1, small oil droplets with radii of tens of microns have small rise speeds and tend to remain suspended in the water. They can become widely dispersed into the water column by turbulent diffusion and be subject to fairly rapid biodegradation. In contrast, large oil droplets of/or blobs or water-in-oil emulsions, with radii of hundreds of microns or larger, will tend to rise to the surface, where the oil can contaminate shorelines, birds, and marine mammals. From the standpoint of oil spill mitigation, small oil droplets are clearly preferred.

Many laboratory studies have been carried out to study droplet generation and emulsion formation (e.g. MacKay and Zagorski, 1982). Usually water and oil are placed in a container and subjected to mechanical agitation. Delvigne and Sweeney (1988, hereafter DS) investigated the breakdown of oil droplets in grid-generated turbulent flows and also in breaking waves generated in laboratory tanks. They found a dependence of the droplet size on oil viscosity and mean energy dissipation rate and hypothesized that small eddies in turbulent flows are responsible for oil droplets splitting because they can cause large shear on the droplets.

Hinze (1955), however, argued that the dynamic pressure forces of turbulent flows are the more likely cause for the droplet breakup. The breakup occurs when the Weber number

$$We = \frac{\rho \overline{q^2} a}{\gamma} \tag{1}$$

exceeds a threshold. Here ρ is the water density, $\overline{q^2}$ the averaged squared velocity difference in the flow over a distance of the droplet radius a and γ the oil–water

*Corresponding author: Institute of Ocean Sciences, P.O. Box 6000, 9860 West Saanich Road, Sidney, B.C. Canada V8L 4B2.

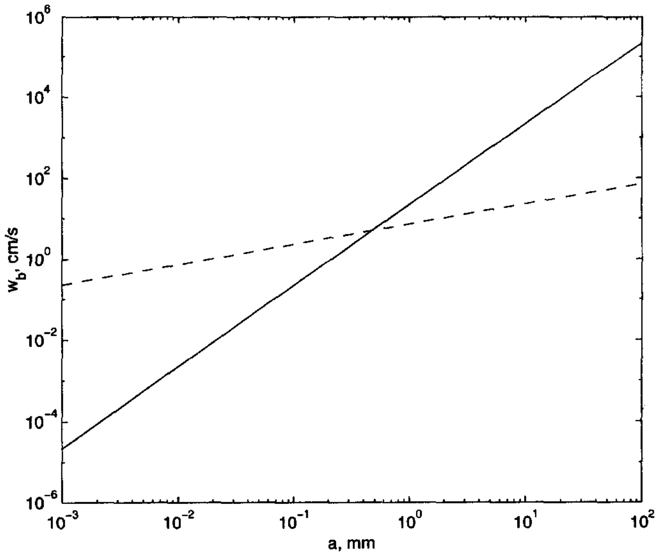

Fig. 1 Buoyancy rise speed of oil droplets with density of 900 kgm^{-3} in water density of 1000 kgm^{-3} (cf. Clift *et al.*, 1978). At small droplet sizes (droplet Reynolds number $Re < 50$, $a < 0.4$ mm), the rise speed varies quadratically with the radius a (solid line). At large droplet sizes ($Re > 50$, $a > 0.4$ mm), the rise speed varies like $a^{1/2}$ (dashed line).

interfacial surface tension coefficient. Using the theory of isotropic homogeneous turbulence to relate velocity fluctuations to mean dissipation rate ε, Hinze obtained a formula for the maximum droplet size (95% of the volume is included in droplets with radius less than $a_{\max}$.)

$$a_{\max} = c(\gamma/\rho)^{3/5}\varepsilon^{-2/5} \tag{2}$$

where $c(\approx 0.363)$ is an empirical constant obtained by calibrating (2) against laboratory observations. Fraser and Wicks (1995) applied the idea of a critical Weber number to calculate oil droplet sizes, but they identified the velocity scale $(\overline{q^2})^{1/2}$ with either the phase speed or water particle velocity of ocean surface waves. Because pressure fluctuations on the scale of droplet radius cause the droplet breakup, Hinze's formula based on the dissipation rate is more appropriate.

Hinze's formula suggests that the droplet size does not depend on the oil viscosity, which is at variance with the experimental data of DS. Moreover, when oil droplets are sufficiently small, the droplet Reynolds numbers will be small and the flows inside the oil droplets will be viscously dominated. Viscous shear rather than pressure must then be the dominant force to overcome the surface tension force (cf. Taylor, 1934). Here we develop an alternative theory for the generation of oil droplets based on the assumption that viscous shear is the mechanism for breakup. Our work is based on research on drop breakup in shear flows (Rallison, 1984; Stone, 1994). A key result which we shall use is the criterion of a critical shear rate above which a drop of a certain radius will disintegrate. We obtain from this criterion an estimate of the size of the largest possible droplets that can survive viscous shear. This formula, as well as Hinze's formula, will first be compared with DS experimental results and then applied to oil spills in the ocean.

A number of oil spill response technologies has been developed to mitigate the effect of oil on the marine environment. One is the use of surface-active chemical dispersants. The surfactants are partly oil soluble, partly water soluble and can reduce the interfacial tension between the oil and water, thus helping to break an oil slick into oil droplets (Doerffer, 1992). However, using chemical dispersants has remained controversial, because the effectiveness of dispersants on different oils over a range of environmental conditions has not been satisfactorily resolved. If the pressure force is the mechanism responsible for droplet breakup in the marine environment, Hinze's formula suggest a rather weak dependence of the droplet size on the interfacial surface tension coefficient. However, if turbulent shear is the droplet breakup mechanism, we shall show that the droplet size depends strongly on the surface tension coefficient. Oil droplets generated from an oil slick treated with chemical dispersants will then be much smaller than those from an untreated oil slick. Alternatively, small oil droplets can be generated from a chemically-treated oil slick in turbulent flows with much weaker dissipation rates.

The plan for this paper is as follows. In the next section we use the Kolmogorov turbulence spectrum to calculate the shear experienced by an oil droplet. We then review research on droplet breakup in shear flows. We present the main theoretical results of this paper in which we propose two hypothetical regimes of oil droplet sizes and compare them with the experimental data of DS. We summarize the measurements of energy dissipation rates in the upper ocean and estimate the size of oil droplets that can be generated by natural breaking waves. The last section discusses the effectiveness of chemical dispersion and gives an estimate of water-in-oil emulsion blob size.

Calculation of Strain Rate in Turbulent Flows

Turbulence consists of eddies of different sizes. Large eddies derive their energy directly from the mean flow and have a size as large as the scale of the mean flow. The energy of large eddies is transferred via an eddy cascade to small eddies where energy is dissipated into heat under the influence of viscosity (Tennekes and Lumley, 1972). While large eddies are responsible for most momentum and scalar transport, it is the small eddies that dominate the shear and are likely to be important for the breakup of droplets in turbulent flows.

The smallest scale of motion in turbulent flows adjusts itself to the value of viscosity. It depends only on the kinematic viscosity ν (m^2 s^{-1}) and on the rate energy is supplied by large-scale motion and then dissipated at small scale ε ($m^2 s^{-3}$). On dimensional grounds, one can form

$$\eta = (\nu^3/\varepsilon)^{1/4}, \tag{3}$$

$$\tau = (\nu/\varepsilon)^{1/2}, \tag{4}$$

$$v = (\nu\varepsilon)^{1/4}, \tag{5}$$

which are Kolmogorov microscales of length (η), time (τ) and velocity (v), respectively (see Batchelor, 1959). Motion at scale η is quite viscous.

The spectral energy density $E(k)$ is defined such that

$$\int_0^{\infty} E(k)\mathrm{d}k = \frac{1}{2}\sum_{i=1}^{3} \overline{u_i^2} \tag{6}$$

is the total kinetic energy per unit mass, k the wavenumber and u_i ($i = 1,2,3$) the components of turbulent velocity fluctuations in three directions. When the Reynolds number is large, there exists an equilibrium range of wave numbers within which the energy density depends only on the viscosity and the amount of energy cascading down the spectrum, i.e. $E = E(k,\varepsilon,\nu)$, which can have only one nondimensional form (see Tennekes and Lumley, 1972):

$$\frac{E(k)}{\nu^{5/4}\varepsilon^{1/4}} = f(k\eta). \tag{7}$$

Most of the viscous dissipation of energy occurs near the Kolmogorov microscale η. The spectrum of the dissipation $D(k)$ is given by

$$D(k) = 2\nu k^2 E(k), \tag{8}$$

and the total dissipation rate ε is given by

$$\varepsilon = 2\nu \sum_{i=1}^{3}\sum_{j=1}^{3} \overline{s_{ij}s_{ij}} = \int_0^{\infty} D(k)\mathrm{d}k \tag{9}$$

in which $s_{ij} = (1/2)(\partial u_j/\partial x_i + \partial u_i/\partial x_j)$ is the rate of strain tensor (see Batchelor, 1967).

Within the equilibrium range of wave numbers, there exists an inertial subrange in which viscous dissipation is negligible. The transfer of energy by vortex stretching is the dominant process. The motion within the inertial subrange is therefore determined uniquely by the rate ε at which energy enters it at the low wavenumber end and leaves it at the high wavenumber end. Dimensional analysis suggests

$$E(k) = \alpha\varepsilon^{2/3}k^{-5/3} \tag{10}$$

(see Tennekes and Lumley, 1972), and experimental data indicate that $\alpha \approx 1.5$.

An oil droplet of size a corresponds to a wavenumber $k_0 = \pi/a$. The approximate total shear experienced by this droplet can be derived from eqn (9) and eqn (10),

$$s(a) = \left(\int_0^{k_0} \alpha\varepsilon^{2/3}k^{1/3}\mathrm{d}k\right)^{1/2}, \tag{11}$$

$$= \frac{(3\alpha)^{1/2}}{2}\varepsilon^{1/3}k_0^{2/3}, \tag{12}$$

$$= \alpha'\varepsilon^{1/3}a^{-2/3}, \tag{13}$$

provided that $2a > \eta$, i.e. if the droplet diameter is greater than the Kolmogorov microscale. Here $\alpha' = (3\alpha)^{1/2}(\pi)^{2/3}/2 \approx 2.3$. We note that $s(k_0) \propto k_0^{2/3}$, i.e. the strain rate imposed on smaller eddies is larger, though larger eddies contain most of the turbulent kinetic energy. We also note that the velocity shear in eddies in the inertial subrange is partitioned equally between the strain rate and vorticity in the statistical mean sense, so that the averaged vorticity and strain rate are of the same order of magnitude.

If $2a < \eta$, the upper limit of the integration must be replaced by $\eta = (\nu^3/\varepsilon)^{1/4}$. Since the energy density spectrum shows a rapid decay at wavenumbers above $2\pi/\eta$, the contribution to the strain rate from $k > 2\pi/\eta$ can be neglected. Thus, for $a < (1/2)\eta$, we have

$$s(a) = \left(\int_0^{2\pi/\eta} \alpha\varepsilon^{2/3}k^{1/3}\mathrm{d}k\right)^{1/2}, \tag{14}$$

$$= 2^{2/3}\alpha'\varepsilon^{1/2}\nu^{1/2}. \tag{15}$$

Criterion for Drop Breakup in Shear Flows

When a drop of one fluid is suspended in a second fluid that is made to shear, the drop will deform, and, if the local shear rate is sufficiently large, it will break into two or more fragments. The principal goals of experimental and theoretical work on this topic have been to discover how much distortion a given flow produces, how strong the flow must be to break up the drop, and the number and size of the droplets that result from a breakup (Acrivos, 1983; Rallison, 1984; Stone, 1994). We are primarily interested in the flow condition causing the drop breakup.

If a drop of the discrete phase is sufficiently small, the Reynolds number of the fluid motion responsible for deforming the drop is low. Thus, inertial forces are negligible. If the length scale of the variation of the imposed flow is much larger than the drop radius, the only external flow term responsible for deforming the drop shape is the local velocity gradient. Hence, one may obtain useful information about drop breakup by considering linear shear flows.

We denote the viscosities of the suspending fluid and the drop as μ and $\mu_d = \lambda\mu$ (and the kinematic viscosities as ν and ν_d), respectively. The corresponding densities are written as ρ and $\rho_d = \kappa\rho$, and the surface-tension coefficient between the two phases is γ. The radius of the undeformed drop is denoted by a. Then if the outer fluid has a shear S, the flow will be viscously dominated inside and near the drop provided that the Reynolds numbers Sa^2/ν and Sa^2/ν_d are both small. The shear flow in a frame of reference moving with the centre of the drop is given by

$$\mathbf{u} = \mathbf{x}\bullet\nabla\mathbf{u} = S(\mathbf{e}+\boldsymbol{\xi})\bullet\mathbf{x} \tag{16}$$

where $\mathbf{e}$ is the normalized rate of strain rate tensor and ξ is the normalized vorticity (Rallison, 1984).

The drop deformation and breakup is determined mainly by three dimensionless numbers: (1) $\lambda = \mu_d/\mu$, the ratio of drop viscosity to that of the suspending fluid; (2) $Ca = \mu Sa/\gamma$, a capillary number representing the ratio of flow forces to surface tension; (3) the relative magnitude of $\mathbf{e}$ and ξ (the flow type). Other factors such as the history of the flow as specified by $\nabla\mathbf{u}(t)$ and the initial shape of the drop could also be relevant (Stone and Leal, 1989), although they will be neglected in the present study.

Since Taylor's (1934) pioneering work, two basic types of shear flow have been studied. Type I is a plane hyperbolic flow with $\mathbf{e} = \mathrm{diag}(1, -1, 0)$ and $\xi = 0$. In this irrotational flow, the drop is stretched in one direction but compressed in the perpendicular direction. Type II is a simple shear flow in which

$$\mathbf{e} = \frac{1}{2}\begin{pmatrix} 0 & 1 & 0 \\ 1 & 0 & 0 \\ 0 & 0 & 0 \end{pmatrix} \text{and } \xi = \frac{1}{2}\begin{pmatrix} 0 & 1 & 0 \\ -1 & 0 & 0 \\ 0 & 0 & 0 \end{pmatrix}$$

such that $|\mathbf{e}|/|\xi| = 1$. A drop placed in the simple shear flow is not only streched in a diagonal direction but also rotates. The difference between the two flow types lies in the vorticity, the effects of which may become important for high viscosity ratio λ. In turbulent flows, the local shear acting on a small drop will in general be a combination of the two flow types.

These studies have focused on predicting the breakup condition. A drop is broken up by the applied shear if

$$Ca = \frac{\mu Sa}{\gamma} > Ca_c. \tag{17}$$

Figure 2(a) shows the critical capillary number Ca_c as a function of viscosity ratio λ for plane hyperbolic flow and Fig. 2(b) for simple shear flow. Drops with either a low or high viscosity ratio are harder to break up than those with $\lambda = O(1)$. When $\lambda \to 0$, as for air bubbles in water or water droplets in water-in-oil emulsions, the asymptotic theory by Hinch and Acrivos (1979), Hinch and Acrivos (1980) shows that

$$Ca_c = 0.145\lambda^{-1/6} \text{ for plane hyperbolic flow,} \tag{18}$$

$$Ca_c = 0.054\lambda^{-2/3} \text{ for simple shear flow,} \tag{19}$$

in excellent agreement with experiment results for λ up to 1. For high viscosity ratios with $\lambda > 10$, such as oil droplets in water, there is no theory, but we can fit an empirical power law

$$Ca_c \approx 0.068\lambda^{1/8} \tag{20}$$

for the plane hyperbolic flow. A viscous drop can be broken up in the plane hyperbolic flow but not in the simple shear flow if $\lambda > 4$. Such a dramatic effect of vorticity was first demonstrated by Taylor (1934), who observed that a drop merely rotated and remained nearly spherical. In the statistical mean sense, small eddies in the equilibrium range have nearly equal partition between the strain rate and vorticity as occurs in simple shear flow. It may thus appear that small rotational eddies are incapable of breaking up highly viscous oil droplets. However, since the stretching of vortices by the strain rate must occur for the energy transfer in turbulence, the strain rate should be effective in causing drop deformation and breakup. Hence, we assume that (20) is applicable for the breakup of oil droplets in any turbulent flow, though it

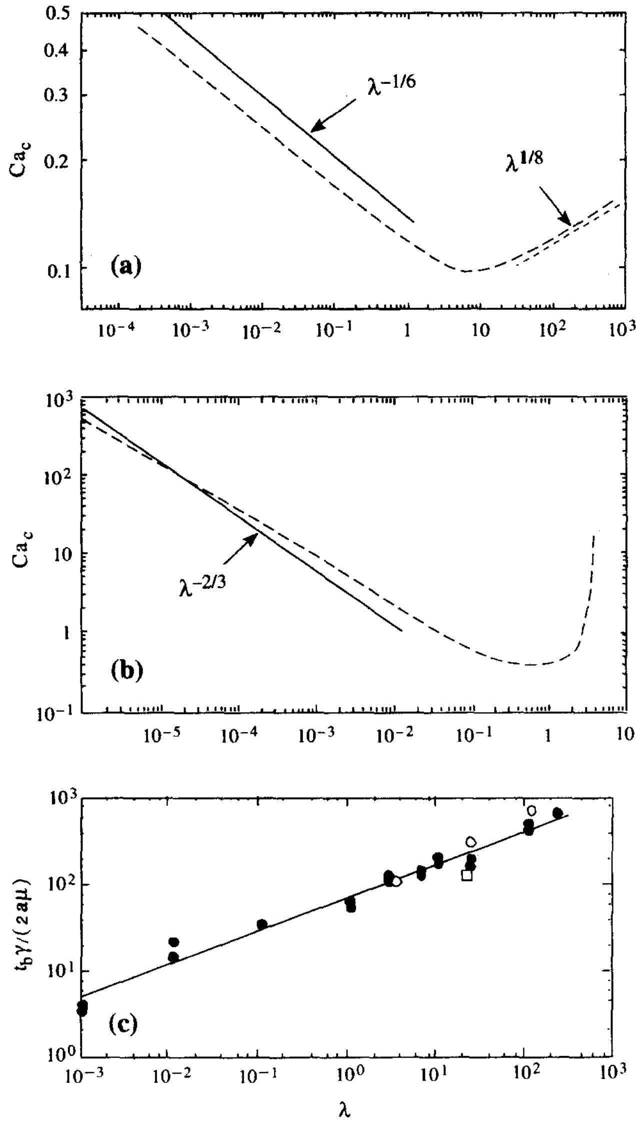

Fig. 2 Critical capillary number Ca_c as a function of viscosity ratio λ in (a) the plane hyperbolic flow and (b) the simple shear flow. The dashed lines are experimental data taken from Grace (1982), the solid lines from the asymptotic theory of Hince and Acrivos (1979) and the dotted line is an empirical fit to Grace data at high viscosity ratio $\lambda > 10$. Modified from Rallison (1984). (c) Time taken for the applied constant shear to break up a drop in the plane hyperbolic flow. The breakup time is nondimensionalized by $2a\mu/\gamma$. Modified from Grace (1982).

is possible that Ca_c may increase with λ more rapidly than that suggested by (20).

The applied shear S has to exceed a critical value in order to overcome the surface tension force that maintains the drop. It also has to be sustained for a time sufficient for the breakup to occur. Figure 2(c) shows that the nondimensionalized breakup time $t_b\gamma/(2a\mu)$ increases with γ (Grace, 1982). The more viscous the drop is, the longer it takes for a given shear flow to break it up. For an oil droplet in water, taking $\gamma = 10^{-2}$ kg s^{-2}, $\mu = 10^{-3}$ kg m^{-1} s^{-1}, $a = 10^{-4}$ m and $\lambda = 100$, we obtain $t_b = O(10^{-2})$ s. This time scale will be compared with the persistence time of an intermittent event of high energy dissipation when we calculate the maximum size of oil droplets.

Determination of Droplet Sizes and Comparison with Laboratory Experiments

The breakup criterion (17) can be used to estimate the maximum size of oil droplets that can withstand turbulent shear, i.e.

$$a_{max} = \frac{Ca_c\gamma}{\mu S}. \tag{21}$$

Substituting (13) or (15) for the strain rate S and (20) for the critical capillary number Ca_c, we obtain from (21) a maximum size; if $2a_{max} \geq \eta$,

$$a_{max} = \alpha_1\left(\frac{\gamma}{\mu}\right)^3 \varepsilon^{-1}\left(\frac{\mu_d}{\mu}\right)^{3/8} \tag{22}$$

where $\alpha_1 = (0.068/\alpha')^3 \approx 2.6 \times 10^{-5}$; and if $2a_{max} < \eta$,

$$a_{max} = \alpha_2\left(\frac{\gamma}{\mu}\right)\nu^{1/2}\varepsilon^{-1/2}\left(\frac{\mu_d}{\mu}\right)^{1/8} \tag{23}$$

where $\alpha_2 = 0.068/(2^{2/3}\alpha') \approx 0.019$. We note that the coefficient 0.068 for the critical Capillary number and α for the turbulent shear spectrum are both empirical constants and any variation in each will result in larger changes in a_{max} because of the cubic dependence.

The distribution of small-scale turbulence is highly non-uniform in space and time and has an intermittent character. Strong turbulent fluctuations tend to concentrate into individual patches surrounded by extensive flow regions in which there are only much smoother large-scale disturbances (Monin and Yaglom, 1975). If turbulent shear associated with intermittent high dissipation events causes the disintegration of oil droplets, we should perhaps use the peak dissipation rate ε_{max} rather than the mean dissipation rate $\bar{\varepsilon}$ when calculating oil droplet sizes. Kolmogorov–Obukhov–Yaglom theory suggests that the dissipation rate is lognormally distributed and spans a wide range of values. If we use Mandelbrot's fractal model of turbulence, we obtain $\varepsilon_{max} = (L/r)^{0.27}\bar{\varepsilon}$ (Sreenivasan and Meneveau, 1986). This would give an intermittency factor of 10 for a droplet of 400 μm in a tube of 4 m height. In formula (2), which gives the maximum size of droplets that can survive turbulent pressure fluctuations, the mean dissipation rate was used. In order to compare (22) or (23) with (2), we shall assume that ε in (22) and (23) is the mean dissipation rate. If we include the intermittency effect and assume $\varepsilon_{max} = 10\bar{\varepsilon}$, we should use $\alpha_1 \approx 2.6 \times 10^{-6}$ in (22) and $\alpha_2 \approx 6 \times 10^{-3}$ in (23).

In the turbulence inertial subrange the differential velocity over a distance a is of order $\varepsilon^{1/3}a^{1/3}$ by use of (13). Thus, we can define two droplet Reynolds numbers as

$$Re_c = \frac{\varepsilon^{1/3}a^{4/3}}{\nu} \tag{24}$$

$$Re_d = \frac{\varepsilon^{1/3}a^{4/3}}{\nu_d} \tag{25}$$

where $Re_c = 1$ at $a = \eta$. The shear formula applies only if the droplet Reynolds numbers are small. When both Reynolds numbers are large, the pressure force is likely the mechanism for droplet breakup and we should use Hinze's formula (2) to calculate the droplet size.

In order to actually break up a droplet, the mechanical shear and hence ε have to persist for a period t_b. We have found little information about the temporal intermittency in the published literature. Nevertheless, we can attempt to estimate a time scale by a dimensional argument. For a patch size r, an associated time scale is proportional to $\varepsilon_r^{-1/3}r^{2/3}$ or 4.6×10^{-2} s for the persistence time of an intermittent event of size $r = 10$ mm and dissipation rate $\varepsilon_r = 1$ m^2 s^{-3}. This is comparable to the breakup time t_b of small drops. Thus, we argue that the intermittent events of high energy dissipation can last long enough to break up the oil droplets.

The two droplet breakup mechanisms suggest that oil droplet sizes have two different regimes, depending on the magnitude of dissipation rate in the turbulent flow. During the early stages of an oil slick breakup, the droplet sizes and Reynolds numbers are large so that pressure forces are necessarily the dominant force of breakup. However, the size of oil droplets that are finally stabilized by the surface tension force depends on whether the pressure or the viscous shear is the operating mechanism during the final stage of breakup. In flows with low energy dissipation rates, pressure force breaks the droplets down to a size stabilized by the surface tension force and the droplet Reynolds numbers remain large throughout the breakup process. In this regime, the final droplet size varies like $\varepsilon^{(-2/5)}$. In flows with high dissipation rates, oil droplets are

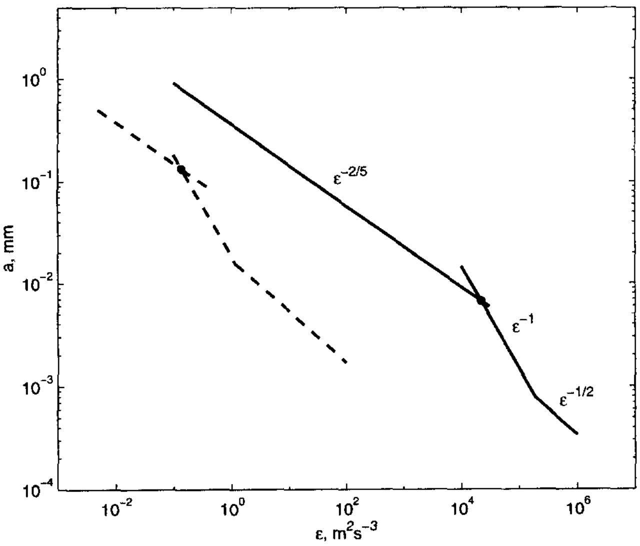

Fig. 3 Two regimes of oil droplet sizes (solid lines) for an example of Prudhoe Bay oil which has dynamic viscosity $\mu_d = 0.1\ \mathrm{kgm}^{-1}\,\mathrm{s}^{-1}$, density $\rho_d = 900\ \mathrm{kgm}^{-3}$ and oil–water interfacial surface tension coefficient $\gamma = 10^{-2}\ \mathrm{kgs}^{-2}$ (cf. DS). The dashed lines correspond to $\gamma = 5\times10^{-4}\ \mathrm{kgs}^{-2}$ when chemical dispersants are used. The solid dots represent the transition points from the pressure regime to the shear regime.

split into smaller sizes. The droplet Reynolds numbers may become sufficiently small so that the viscous shear takes over the pressure force in determining droplet breakup. In this regime the final droplet size varies as $\varepsilon^{(-1)}$ for $2a > \eta$ [see (22)] and switches to $\varepsilon^{(-1/2)}$ for $2a < \eta$ [see (23)]. Figure 3 shows the two hypothetical regimes of droplet sizes for an example of Prudhoe Bay oil.

Using the formulae (2) and (22), we obtain a dissipation rate, ε_c, at the transition between the pressure and shear regimes,

$$c\left(\frac{\gamma}{\rho}\right)^{3/5}\varepsilon_c^{(-2/5)} = \alpha_l\left(\frac{\gamma}{\mu}\right)^3\varepsilon_c^{(-1)}\left(\frac{\mu_d}{\mu}\right)^{3/8}, \tag{26}$$

or

$$\varepsilon_c = \left(\frac{\alpha_l}{c}\right)^{5/3}\left(\frac{\gamma}{\mu}\right)^5\left(\frac{\gamma}{\rho}\right)^{-1}\left(\frac{\mu_d}{\mu}\right)^{5/8}. \tag{27}$$

Substituting this into (2) or (22) gives a corresponding droplet size

$$a_c = \alpha_l\left(\frac{\alpha_l}{c}\right)^{-5/3}\left(\frac{\gamma}{\mu}\right)^{-2}\left(\frac{\gamma}{\rho}\right)\left(\frac{\mu_d}{\mu}\right)^{-1/4} \tag{28}$$

and a droplet Reynolds number

$$Re_d = \varepsilon_c^{1/3}a_c^{4/3}/\nu_d = \alpha_l^{-1/3}c^{5/3}\left(\frac{\rho_d}{\rho}\right)\left(\frac{\mu_d}{\mu}\right)^{-9/8}. \tag{29}$$

In the shear regime, if the droplet size is smaller than the Kolmogorov microscale, i.e. $2a < \eta$, the droplet size is given by (23). The transition from (22) to (23) occurs when

$$2a_{\max} = 2\alpha_l\left(\frac{\gamma}{\mu}\right)^3\varepsilon_k^{-1}\left(\frac{\mu_d}{\mu}\right)^{3/8} = \eta = \left(\frac{\nu^3}{\varepsilon_k}\right)^{1/4}, \tag{30}$$

or

$$\varepsilon_k = (2\alpha_l)^{4/3}\left(\frac{\gamma}{\mu}\right)^4\left(\frac{\mu_d}{\mu}\right)^{1/2}\nu^{-1}. \tag{31}$$

These theoretical results are now compared with the experimental results of DS. Homogeneous turbulence with different energy levels was generated by an oscillating grid in a vertical tube 4 m high and 0.3 m wide. DS derived the mean energy dissipation rates from calculations using the hydraulic resistance of the oscillating grid. Oil droplets of size about 1 cm and covering a wide range of oil types were introduced into the grid column at various inlets. Oil–water samples were withdrawn from the grid column and led through a laser-beam particle sizer to determine the drop size distribution. Figure 4 summarizes the experimental results. For mean dissipation rate ε exceeding $0.1\ \mathrm{m}^2\,\mathrm{s}^{-3}$, DS fit an empirical relation between the mean and maximum droplet sizes and the mean energy dissipation rate and the oil viscosity,

$$\bar{a}, a_{\max} \propto \varepsilon^{(-0.5)}\mu_d^{0.34} \tag{32}$$

DS used two types, one of which is the Prudhoe Bay oil (PB). This oil has dynamic viscosity $\mu_d = 0.1\ \mathrm{kgm}^{-1}\,\mathrm{s}^{-1}$, density $\rho_d = 900\ \mathrm{kgm}^{-3}$ and oil–water surface tension coefficient $\gamma = 10^{-2}\ \mathrm{kgs}^{-2}$ (the oil properties depend on temperature and the amount of weathering experienced; here we choose typical values). The water density is taken to be $\rho = 1000\ \mathrm{kgm}^{-3}$. For this oil, we calculate from (27), (28) and (29) the dissipation rate at the transition between the two regimes $\varepsilon_c \approx 2.2\times10^4\ \mathrm{m}^2\,\mathrm{s}^{-3}$, the droplet size $a_c \approx 6.7\ \mu\mathrm{m}$ and the droplet Reynolds number $Re_d \approx 0.03$. Assuming an intermittency factor of 10, i.e. $\alpha_l = 2.6\times10^{-6}$, we obtain $\varepsilon_c \approx 474\ \mathrm{m}^2\,\mathrm{s}^{-3}$, $a_c \approx 31\ \mu\mathrm{m}$ and $Re_d \approx 0.06$. Thus, it appears that all DS data shown in Fig. 4(a) fall into the Hinze regime. Comparing DS empirical formula with Hinze's formula, we find similar power law dependence on the dissipation rate. However, Hinze's formula suggests that the droplet size should be independent of the oil viscosity while the DS experiments show that more viscous oil droplets are larger. Nevertheless the transition between the pressure and shear regimes is not expected to be abrupt. It is quite possible that viscous effects may become significant even when the dissipation rate is less than ε_c.

Eqn (2) and eqn (22) [or eqn (23)] provide an estimate for the largest possible droplet sizes. Droplets with slightly larger sizes are broken into many satellite droplets which can be one or two orders of magnitude smaller (Tjahjadi and Ottino, 1991; Tjahjadi *et al.*, 1992). Therefore, there will be a range of stable droplet sizes in a turbulent flow. Figure 4(c) gives examples of droplet size distribution measured in the DS experiments, which shows a power-law distribution $N(a) \propto a^{-2.3}$ where $N(a)$ is the number of droplets in a unit size interval Δa around a. This size distribution is fairly close to the a^{-3} spectrum obtained in experiments on controlled drop breakup in two-dimensional time-periodic chaotically advected flows (Muzzio *et al.*, 1991). The a^{-3} spectrum suggests a self-similarity in drop size distribution and is related to the self-similar distributions of stretching rates and local capillary numbers in chaotic flows.

Relevance to Oceanic Turbulent Flows Generated by Breaking Waves

According to field observations, most oil droplets permanently dispersed into the ocean are in the size range between 1 and 70 μm, with a median size of 20 μm (Lunel, 1993). We now discuss typical values of

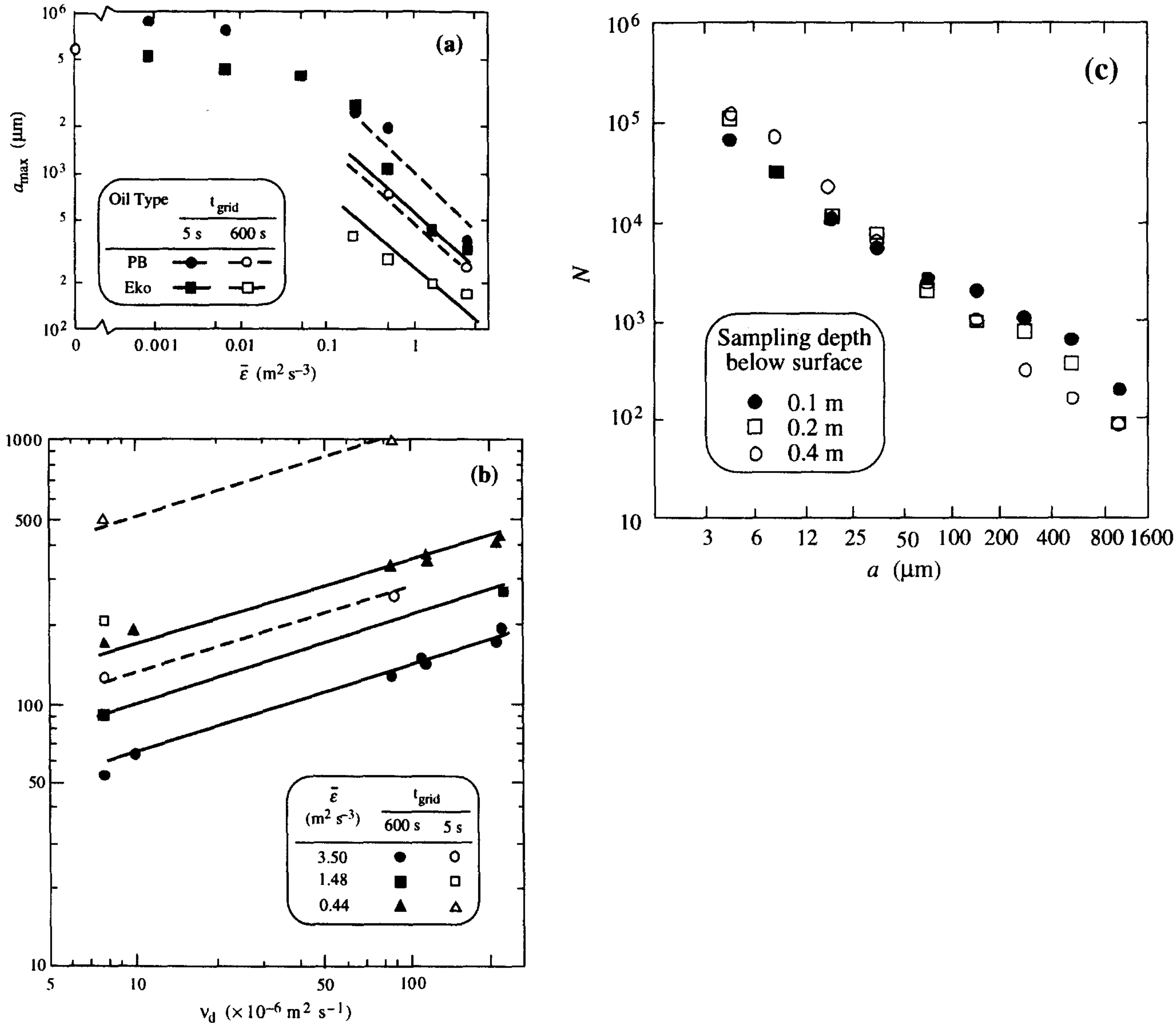

Fig. 4 Laboratory results on the breakup of oil droplets. Both Prudhoe Bay oil (PB) with medium viscosity and Ekofisk oil (Eko) with low viscosity were used. The grid was oscillated for a period $t_{grid} = 5$ s to simulate a short-duration turbulence of breaking waves and for $t_{grid} = 600$ s to obtain a steady-state droplet size distribution. (a) Maximum droplet size a_{max} as a function of the mean energy dissipation rate ε. (b) Mean droplet size $\bar{a}$ as a function of oil kinematic viscosity. (c) Droplet size distribution $N(a)$ versus a. Modified from Delvigne and Sweeney (1988).

ε in the surface water of the ocean to examine whether the turbulent flow is sufficiently energetic to generate these small oil droplets.

In wall-bounded turbulent flows, there exists a log layer adjacent to the solid boundary (apart from a thin viscous sublayer), in which the mean velocity varies logarithmically and the averaged dissipation rate $\varepsilon = u_*^3/(\kappa z)$ varies inversely with distance from the boundary. Here $u^* = (\tau_w/\rho)^{1/2}$ is the water friction velocity representing the magnitude of wind stress τ_w and $\kappa \approx 0.4$ is the von Karman constant (Hinze, 1975). Under conditions of wave breaking, however, ε exceeds that of the log layer by one to two orders of magnitude in the surface water, as shown in Fig. 5(a) (Agrawal *et al.*, 1992). The region of strong dissipation extends from a depth $d_c = \beta H_s$ to a few metres, where H_s is the significant wave height and $\beta = (1.2$ to $1.6)$ is a scaling factor depending on the sea state. Within a surface layer of thickness d_c, ε is approximately constant. From Fig. 5(a), $\varepsilon\kappa z/u_*^3 \approx 100$ at $gz/u_*^2 = 10^4$, so for $u_* = 0.01\ \mathrm{m\ s^{-1}}$ we obtain $\varepsilon \approx 2.5 \times 10^{-3}\ \mathrm{m^2\ s^{-3}}$. Open ocean measurements by Gemmrich (1997) show a similar order of magnitude for the mean dissipation rates. These mean dissipation rates, averaged over a long time record, are useful in describing the mean state of turbulent flows in the upper ocean, but may not be relevant to the highly energetic breaking wave events that are responsible for the breakup of oil droplets.

Agrawal *et al.* (1992) showed that the turbulence generated by breaking waves is temporally intermittent. Fig. 5(b) is a time series of ε_t averaged over a sampling period of 13 s in a 80-min long record. Clearly ε_t is an order of magnitude larger than the averaged value, i.e. $\varepsilon_t = O(10^{-2})$ to $O(10^{-1})\ \mathrm{m^2\ s^{-3}}$ in breaking waves. Since the sampling time 13 s is much longer than the drop breakup time scale t_b, the instantaneous value of ε may show a even larger fluctuation about its time average. It is possible that ε_t averaged over a shorter period may reach $O(1)\ \mathrm{m^2\ s^{-3}}$.

Other studies of turbulence dissipation in breaking waves suggest a similar magnitude for ε. Duncan (1981) made laboratory measurements on the rate of energy loss per unit crest length from a quasi-steady breaking wave produced by a subsurface hydrofoil. The estimated energy loss rate

$$\varepsilon_l = (0.044 \pm 0.008)\rho c_b^5/g \tag{33}$$

increases rapidly with the phase speed of the breaking wave, c_b. Thorpe (1993) demonstrated that $c_b/c_0 = 0.25$ in which c_0 is the phase speed of the dominant wave. For example, if the dominant wave has a period of $T_w = 4$ s and a length of $L_w = 16$ m, we then have $c_0 = 6.3\ \mathrm{m\ s^{-1}}$ and $c_b = 1.6\ \mathrm{m\ s^{-1}}$. Substituting this into

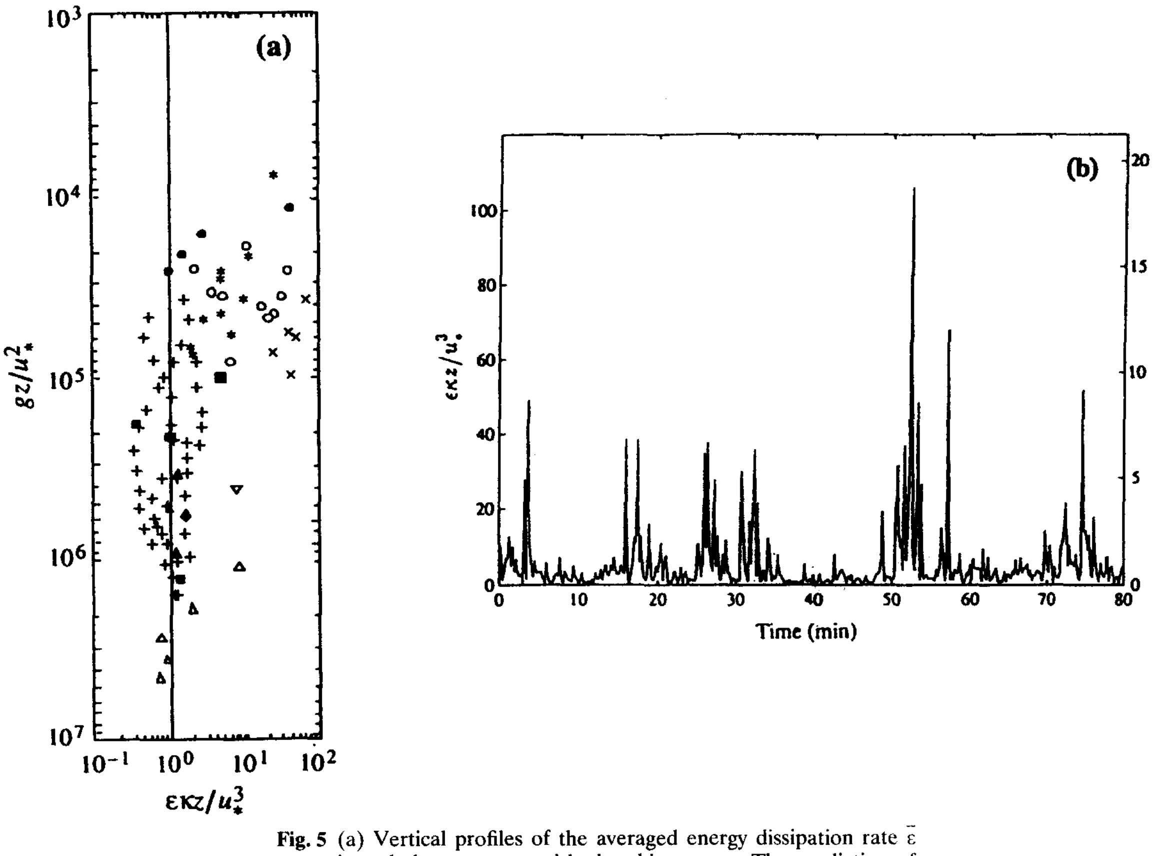

Fig. 5 (a) Vertical profiles of the averaged energy dissipation rate $\bar{\varepsilon}$ in turbulence generated by breaking waves. The prediction of wall-layer theory appears as the vertical line. (b) Temporal intermittency of ε_t in breaking waves. From Agrawal *et al.* (1992).

(33) produces $\varepsilon_l = 50\,\text{kg m}^{-1}\,\text{s}^{-1}$. Thus, the mean energy dissipation rate per unit mass $\varepsilon = \varepsilon_l/\rho(qL_w)^2 = O(10^{-4})$ to $O(10^{-3})\,\text{m}^2\,\text{s}^{-3}$ where $q<1$ is the percentage of whitecap coverage over one wavelength. However, the energy dissipation rate in unsteady breaking waves can be an order of magnitude smaller than steady breakers (Melville, 1994). In laboratory measurements, Rapp and Melville (1990) found that more than 90% of the total energy lost from the wave field was dissipated within four wave periods after the inception of breaking. This suggests the duration of high energy dissipation in breaking waves to be about 20 s.

Taking these studies together, we may conclude that typical values of energy dissipation rate in breaking waves range from $0.1\,\text{m}^2\,\text{s}^{-3}$ in moderate sea conditions to $10\,\text{m}^2\,\text{s}^{-3}$ in stormy sea conditions. As shown in Fig. 3, the pressure force must then be the breakup mechanism and can generate oil droplets with radius of $O(100)\,\mu\text{m}$. These oil droplets have relatively large buoyancy rise speeds and may not remain dispersed into the water column. We conclude that natural breaking waves cannot cause a significant amount of droplet dispersion except in extreme weather conditions where the dissipation rates may be much larger than those estimated here.

Implications for Chemical Dispersion and Water-in-oil Emulsions

As alluded in the introduction, chemical dispersants have often been used to treat an oil slick in order to facilitate the generation and dispersion of oil droplets. Laboratory experiments on chemical dispersion indicated a considerable shift in droplet sizes to smaller values and consequently a greater portion of the oil is brought into a long lasting oil dispersion (Delvigne, 1991). Despite considerable testing in the laboratory and in the field, the effectiveness of chemical dispersants over a range of environmental conditions remains unsettled. Let us discuss this issue in light of the theoretical development in Section 4.

After an oil slick is sprayed with chemical dispersants, the oil–water interfacial surface tension is much reduced, usually by a factor of 20 (cf. Fraser and Wicks, 1995). When the stabilizing surface tension force is weakened, oil droplets can be broken down to smaller sizes. However, Hinze's formula (2) and the shear formula (22) and (23) suggest rather different responses of droplet size to reduction in γ. When the pressure force is the dominant breakup mechanism, the droplet size varies like $\gamma^{3/5}$. Suppose chemical dispersants reduce γ by 20 times, the droplet size is only reduced by a factor of 6. However, when the viscous shear is the dominant breakup mechanism, droplet size varies like γ^3 for $2a > \eta$ and γ for $2a < \eta$. A 20 times reduction in γ would result in 8000 or 20 times decrease in the droplet size.

More importantly, the transition between the pressure and shear regimes shifts to a much lower dissipation rate. According to (27)–(29), when γ is reduced by a factor of 20 times, the transition occurs at $\varepsilon_c = 0.14\,\text{m}^2\,\text{s}^{-3}$, $a_c = 134\,\mu\text{m}$ and $Re_d = 0.03$ (see the dashed lines in Fig. 3). In Section 5, we estimated that typical dissipation rates in breaking waves range from 0.1 to $10\,\text{m}^2\,\text{s}^{-3}$. Hence, viscous shear is likely to be the dominant mechanism for generating oil droplets in the ocean when chemical dispersants are used. Furthermore, the oil droplets are mostly in the range $O(10)\,\mu\text{m}$ [with buoyancy rise speeds at $O(10^{-3})$ to $O(10^{-2})$ cm/s] and can thus be permanently dispersed into the ocean.

Breakup of water-in-oil emulsions

Water-in-oil emulsions are difficult to remove and resist degradation but they frequently appear in oil spills. Stable emulsions usually have viscosity over three orders of magnitude larger than the crude oil (Fingas *et al.*, 1995), but the oil–water interfacial surface tension coefficient may be reduced to a half (Doerffer, 1992). Although emulsions do not have the properties of a Newtonian fluid, we can tentatively use the formulae of droplet sizes to estimate the largest possible emulsion blobs. For an energy dissipation rate of $10\,\text{m}^2\,\text{s}^{-3}$ and emulsion viscosity $\mu_d = 100\,\text{kgm}^{-1}\,\text{s}^{-1}$, we calculate from (22) a blob size $a = 24.4$ mm. The corresponding droplet Reynolds number is $Re_d = 0.15$. Clearly viscous shear is the mechanism for disintegrating highly viscous water-in-oil emulsions.

Conclusion

In this paper we have attempted to provide a theoretical basis to intepret the laboratory results on the breakup of oil droplets in turbulent flows. In particular, we have derived an alternative formula for maximum droplet sizes based on the hypothesis that turbulent shear is a dominant force for droplet breakup.

Typical dissipation rates in the upper ocean can generate oil droplets of hundreds of microns in size. These droplets have relatively large buoyancy rise speeds and will probably rise to the surface after being injected into the water. In order to generate smaller oil droplets, much larger dissipation rates are required. Since our knowledge of spatial and temporal intermittency of upper ocean turbulence is rather limited, further measurements of turbulent energy dissipation in breaking waves are required, particularly in rough seas. Our results are not inconsistent with the observation that the loss of oil by natural dispersion of oil droplets usually accounts for a small percentage of total volume of the spilt oil (Fingas, 1994). In spills which occurred in extreme weather conditions, such as the *Braer* incident, however, a large percentage of the spilt oil (about 44% in the *Braer* spill) may have been dispersed into the water column by upper ocean turbulent flows. It is also possible that the droplet dispersion was enhanced by the use of chemical dispersants after the spill. Using chemical dispersants shifts the droplet breakup from the pressure regime to the viscous shear regime (see Fig. 3). With sizes at $O(10)$ μm, these oil droplets can remain suspended in the water column.

We have also shown that chemical dispersants help reduce the droplet size when viscous shear is the dominant breakup mechanism. Oil droplets of tens of microns in size can be generated in moderate to stormy sea conditions. This paper suggests that chemical dispersants are effective in promoting permanent dispersion of small oil droplets into the water column.

We thank David Farmer, Konstantin Zahariev, Shafei Zeiden, Bob Stewart and Zhendi Wang for useful discussions and R. Rutka for preparation of diagrams. This work is supported by a Canadian NSERC (Natural Sciences and Engineering Research Council) strategic grant.

Acrivos, A. (1983) The breakup of small drops and bubbles in shear flows. *4th Int. Conf. on Physicochemical Hydrodynamics. Ann. N.Y. Acad. Sci.* **404**, 1–11.

Agrawal, Y. C., Terray, E. A., Donelan, M. A., Hwang, P. A., Williams III, A. J., Drennan, W. M., Kahma, K. K. and Kitaigorodskii, S. A. (1992) Enhanced dissipation of kinetic energy beneath surface waves. *Nature* **359**, 219–220.

Batchelor, G. K. (1959) *The Theory of Homogeneous Turbulence*. Cambridge University Press.

Batchelor, G. K. (1967) *An Introduction to Fluid Dynamics*. Cambridge University Press.

Bobra, M., Fingas, M. and Tennyson, E. (1992) When oil spills emulsify. *Chemtech* **22**, 236–241.

Clift, R., Grace, J. R. and Weber, M. E. (1978) *Bubbles, Drops and Particles*. Academic Press, New York.

Delvigne, G. A. L. (1991) On scale modeling of oil droplet formation from spilled oil. *Proceedings of 1991 Oil Spill Conference*, 501–526.

Delvigne, G. A. L. and Sweeney, C. E. (1988) Natural dispersion of oil. *Oil Chem. Pollu.* **4**, 281–310.

Doerffer, J. W. (1992) *Oil Spill Response in the Marine Environment*. Pergamon Press Ltd., Oxford.

Duncan, J. H. (1981) An investigation of breaking waves produced by a towed hydrofoil. *Proc. Royal Soc. A* **377**, 331–348.

Fingas, M. F. (1994) Chemistry of oil and modelling of spills. *J. Adv. Mar. Tech. Conf.* **11**, 41–63.

Fingas, M. F., Fieldhouse, B., Gamble, L. and Mullin, J. (1995) Studies of water-in-oil emulsions: stability classes and measurement. *Proc. 18 AMOP*, 21–42.

Fraser, T. P. and Wicks III, M. (1995) Estimation of maximum stable oil droplet sizes at sea resulting from natural dispersion and from use of a dispersant. *Proc. 18 AMOP*, 313–316.

Gemmrich, J. R. (1997) A study of turbulence and fine scale temperature variability of the ocean thermal boundary layer under breaking surface waves. PhD thesis, University of Victoria.

Grace, H. P. (1982) Dispersion phenomena in high viscosity immiscible fluid systems and application of static mixers as dispersion devices in such systems. *Chem. Eng. Commun.* **14**, 225–277.

Hinch, E. J. and Acrivos, A. (1979) Steady long slender droplets in two-dimensional straining motion. *J. Fluid Mech.* **91**, 401–414.

Hinch, E. J. and Acrivos, A. (1980) Long slender drops in a simple shear flow. *J. Fluid Mech.* **98**, 305–328.

Hinze, J. O. (1955) Fundamentals of the hydrodynamic mechanism of splitting in dispersion processes. *A.I.Ch.E. Journal* **1**, 289–295.

Hinze, J. O. (1975) *Turbulence*. McGraw-Hill Inc., New York.

Hoult, D. P. (1972) Oil spreading on the sea. *Annu. Rev. Fluid Mech.* **4**, 341–368.

Lunel, T. (1993) Dispersion: oil droplet size measurement at sea. *Proc. 16 AMOP*, 1023–1057.

MacKay, D. and Zagorski, W. (1982) *Studies of Water-in-Oil Emulsions*. Environment Canada Manuscript Report EE-34, Ottawa, Ontario.

Melville, W. K. (1994) Energy dissipation by breaking waves. *J. Phys. Oceanogr.* **24**, 2041–2049.

Monin, A. S. and Yaglom, A. M. (1975) *Statistical Fluid Mechanics: Mechanics of Turbulence*. The MIT Press, MA.

Muzzio, F. J., Tjahjadi, M. and Ottino, J. M. (1991) Self-similar drop-size distributions produced by breakup in chaotic flows. *Physical Review Letters* **67**, 54–57.

Rallison, J. M. (1984) The deformations of small viscous drops and bubbles in shear flows. *Annu. Rev. Fluid Mech.* **16**, 45–66.

Rapp, R. J. and Melville, W. K. (1990) Laboratory measurements of deep-water breaking waves. *Phil. Trans. Royal Soc. London Ser. A* **331**, 735–800.

Schramm, L. L. (1992) Petroleum emulsions: basic principles. In *Emulsions Fundamentals and Applications in the Petroleum Industry*, ed. L. L. Schramm, pp. 1–49. American Chemical Society, Washington, DC.

Sreenivasan, K. R. and Meneveau, C. (1986) The fractal facets of turbulence. *J. Fluid Mech.* **173**, 357–386.

Stone, H. (1994) Dynamics of drop deformation and breakup in viscous fluids. *Annu. Rev. Fluid Mech.* **26**, 65–102.

Stone, H. and Leal, L. G. (1989) The influence of initial deformation on drop breakup in subcritical time-dependent flows at low Reynolds numbers. *J. Fluid Mech.* **206**, 223–263.

Taylor, G. I. (1934) The formation of emulsions in definable fields of flows. *Proc. Royal Soc. A* **146**, 501–523.

Tennekes, H. and Lumley, J. L. (1972) *A First Course in Turbulence*. The MIT Press, MA.

Thorpe, S. A. (1993) Energy loss by breaking waves. *J. Phys. Oceanogr.* **23**, 2498–2502.

Tjahjadi, M. and Ottino, J. M. (1991) Stretching and breakup of droplets in chaotic flows. *J. Fluid Mech.* **232**, 191–219.

Tjahjadi, M., Stone, H. A. and Ottino, J. M. (1992) Satellite and subsatellite formation in capillary breakup. *J. Fluid Mech.* **243**, 297–317.